ELSEVIER

Physica D 99 (1996) 369–380

PHYSICA D

Scaling laws and dissipation scale of a passive scalar in fully developed turbulence

G. Ruiz-Chavarria [a,b,*], C. Baudet [a], S. Ciliberto [a,c]

[a] *Ecole Normale Supérieure de Lyon, Laboratoire de Physique, C.N.R.S. URA 1325, 46 Allée d'Italie, 69364 Lyon, France*
[b] *Departamento de Física, Facultad de Ciencias, UNAM, 04510 México DF, Mexico*
[c] *Departement of Physics, University of Florence, Largo E. Fermi, 50125 Firenze, Italy*

Received 5 February 1996; revised 7 May 1996; accepted 28 May 1996
Communicated by U. Frisch

Abstract

The scaling laws of the temperature structure functions and their relation with those of velocity have been experimentally studied. The relationship between the dissipative scales for velocity and the temperature is first investigated. In agreement with recent numerical simulations of Pumir (1994), it is found that, for Prandtl number close to 1, the dissipation scale for a scalar is smaller than that of velocity. Thus temperature structure functions present a larger scaling interval than that of the velocity. The intermittent corrections of scaling are then analyzed. It is shown that, as proposed in literature (R. Benzi et al., 1992), the second-order structure function is affected only by the velocity intermittency. This structure function is then used as the reference for testing the applicability of the extended self-similarity (ESS) to the passive scalar case. ESS holds, but in a narrower interval than that observed in velocity statistics. Finally, a hierarchy for the temperature structure functions, similar to that proposed by She and Leveque (1994) for the velocity field, is introduced and experimentally tested.

PACS: 47.27Gs; 05.40+j
Keywords: Isotropic turbulence; Self-similarity; Random processes; Passive scalar

1. Introduction

The capacity of the turbulent motion to diffuse for example heat or a contaminant through a fluid is interesting from both a theoretical or a practical point of view.

The basic equation of the advection of a passive scalar θ by a velocity field $\boldsymbol{u}$ is

$$\frac{\partial \theta}{\partial t} + (\boldsymbol{u} \cdot \nabla)\theta = \chi \nabla^2 \theta, \tag{1}$$

where χ is the thermal difussivity. Notice that this equation is linear, but a coupling between θ and $\boldsymbol{u}$ is present via the term $(\boldsymbol{u} \cdot \nabla)\theta$. A random behavior of the scalar is expected to appear when θ is already stochastic at the initial time or when the interaction between θ and $\boldsymbol{u}$ do so.

Recently new trends in passive scalar research has been open. For example Villermaux and Gagne [1] have studied the line dispersion in homogeneous turbulence. The closure of the temperature increment statistics have been also recently analyzed both theoretically [2] and experimentally [3]. The probability

* Corresponding author.

PII S0167-2789(96)00165-0

distribution function of a scalar has been instead analyzed by Castaing [4].

Pumir [5] made a numerical investigation on the small scale structure, in particular he found that there exist narrow sheets where pronounced scalar jumps are observed. This feature is related to the intermittency and it is in conflict with the classical picture by Obukhov and Corrsin [6,7].

Among the different analysis which may be eventually performed [2–12], the statistical properties of homogenous and isotropic turbulence are often investigated by studying the structure functions. The n-order structure function for temperature and velocity are defined as follows:

$$\begin{aligned} R_n(r) &= \langle|\theta(x+r)-\theta(x)|^n\rangle, \\ S_n(r) &= \langle|V(x+r)-V(x)|^n\rangle, \end{aligned} \tag{2}$$

where $\langle\cdots\rangle$ stands for ensemble average, r is a distance, V the velocity component parallel to r and θ is the temperature. One observes that there exists a range in r, called the inertial range, where $S_n(r)$ and $R_n(r)$ have a power law behavior, that is

$$S_n(r) \propto r^{\zeta(n)}, \tag{3}$$

$$R_n(r) \propto r^{\xi(n)}. \tag{4}$$

The inertial range corresponds to lengths where viscosity or diffussivity are negligeable, that is, $L \gg r \gg \eta'$, where η' is the dissipative scale and L is the integral scale at which the energy is injected. For velocity field η' is the Kolmogorov scale $\eta = (\nu^3/\overline{\epsilon})^{1/4}$ (here $\overline{\epsilon}$ is the mean energy dissipation and ν is the kinematic viscosity). Instead for a passive scalar η' is η_θ which is in general different from η. At this level the only conclusion, we can reach, is the following:

$$\eta_\theta = \eta f(Pr), \tag{5}$$

where f is an arbitrary function of the Prandtl number $Pr = \nu/\chi$. In Section 3 some possibilities are analyzed and a comparison with experimental data is made.

Following a parallel with the Kolmogorov ideas for velocity statistics [13], a universal behavior is expected to occur at lengths far away from both the dissipative and the integral scales. Turbulence is seen as a hierarchy of structures of different sizes. First the temperature fluctuations are injected at largest scales, then a cascading is established consisting of a transfer of these fluctuations to increasingly smaller scales until the thermal diffusivity becomes important. If L and η_θ are well separated then a self-similar regime is attained at intermediate scales.

In the classical theory by Obukhov and Corrsin [7] it is assumed that statistical properties of a passive scalar depends solely upon χ, ν, $\overline{\epsilon}$ and $\overline{N}$ ($\overline{N}$ is the mean of the dissipation of the temperature fluctuations, that is: $\overline{N} = \langle\chi \sum_{i=1}^{3}(\partial\theta/\partial x_i)^2\rangle$). This yields to the scaling of the structure functions

$$R_n(r) = C_n \overline{\epsilon}^{-n/6} \overline{N}^{n/2} r^{n/3}. \tag{6}$$

However the $\xi(n)$ exponents are experimentally found different from this theoretical prediction. In fact, the third-order structure functions exhibits approximately a deviation of 20% with respect to that model and the difference is about 45% for the sixth-order structure function. This phenomenon is believed to be produced by the intermittencies of $\overline{\epsilon}$ and $\overline{N}$. The purpose of this paper is to analyze these intermittent properties of a passive scalar, by studying the scaling of the temperature structure functions. We are also interested in studying the dissipation scales which determine the extension of the scaling range of the structure functions.

The paper is organized as follows. In Section 2 the experimental setup is described. Section 3 is devoted to investigate the dissipative scales for velocity and temperature and a comparison with three models is made. In Section 4 the influence of the intermittency of the kinetic energy dissipation and N will be analyzed and a model recently introduced by Benzi et al. [14] will be tested. According to the latter, the second-order structure function $R_2(r)$ is not affected by the intermittency of N, but only by that of ϵ. Another important issue treated in this work is the applicability of extended self-similarity (ESS) [15] to a passive scalar (Section 5). This property was originally discovered in the velocity statistics. It consists of a self-similar behavior of a broader range than the inertial one when the variable r is replaced by $S_3(r)$. In the context of temperature, ESS is studied by plotting $R_n(r)$ vs. $R_2(r)$.

In Section 6 a hierarchy of the temperature structure functions is proposed. The underlying idea is the same as She and Lêveque discussed in a recent paper [16]. Finally conclusions are given in Section 7.

2. Experimental setup

In order to answer the above-mentioned questions concerning the statistics of a passive scalar some measurements were carried out. The experimental setup consists of a wind tunnel with a cross section $50 \times 50\,\mathrm{cm}^2$ and 3 m long. The turbulence is generated with a cylinder of diameter $L = 10\,\mathrm{cm}$. The mean velocity in the tunnel was varied in the range $1.4\,\mathrm{m/s} < U_0 < 6.7\,\mathrm{m/s}$, then the Reynolds number ($Re = U_0 L/\nu$) was in the range $9000 < Re < 45\,000$ corresponding to R_λ (based on the Taylor microscale) in the range $130 < R_\lambda < 470$. In order to produce the temperature fluctuations the air was heated electrically after the cylinder by an array of parallel fine wires whose thickness was about 0.1 mm. This array permits an effectively mixing of heat and does not produce any mean temperature gradient. This heating array is reported in other experiments on turbulent mixing of temperature [8,17] and it is known as mandoline. The wires of mandoline are too fine to disturb the flow. The mandoline was heated with a DC power supply reaching a power of approximately 1 kw, so the increase of mean temperature was between 1°C and 4°C depending on the mean velocity.

In order to measure simultaneously velocity and temperature two probes were placed at a distance less than 1 mm apart. The temperature probe is a platinum wire of diameter 1 μm and 0.3 mm long, with a resistance of 45Ω at 20°C; it works as a cold wire. The current passing in the probe was 0.35 mA, giving a good sensitivity to temperature fluctuations (about 50 μV/°C) and a negligeable one to velocity. The sensor used to measure velocity is a thin wire of diameter 25 μm and 0.5 mm long working as hot wire. In almost all the experiments the size of probes was in the proximity of the dissipative scale, then the statistics in the inertial range is well resolved. The probes were placed at 25 L downstream the cylinder and the temperature sensor was in the lower position. This is made to prevent the air heated by the velocity probe from reaching the platinum sensor.

The instantaneous velocity and temperature were transformed into voltage signals with a TSI anemometer and a Wheatstone bridge, respectively, filtered at a frequency $f_c > U/5\eta$ and digitized with a 16 bits a/d converter. Before filtering, the temperature signal was amplified by a factor 10 000 using a differential amplifier. Time series of at least 7×10^6 points have been recorded which allows us to compute with a statistical accuracy of a few per cent till the 8 order structure function. The local-time measurements are transformed in spatial measurements by using the Taylor hypothesis, that is $r = U_0 \cdot t$. Finally the anemometer output has been corrected to take into account the non-linear response of the hot wire.

3. Dissipative scale

In Section 1, we have already mentioned that in fully developed turbulence the extension of the scaling range of structure functions is determined by the dissipation scale which is a function of Re. This can be seen in Fig. 1 where the R_n are reported as a function of r for different n and Re. A scaling region is observed only for the highest Re, that is, for the smallest dissipative scale. For the velocity structure function the dissipative length scale is the Kolmogorov scale η whereas for the temperature structure functions several hypotheses have been made.

By a dimensional analysis and assuming a dependence on χ and $\bar{\epsilon}$ alone, Monin and Yaglom [6] give an estimate of the dissipative scale for temperature

$$\eta_\theta = (\chi^3/\bar{\epsilon})^{1/4}. \tag{7}$$

Notice that η_θ is simply obtained by replacing ν by χ in the definition of η. Eq. (7) can be written in terms of η, that is

$$\eta_\theta = \eta\, Pr^{-3/4}. \tag{8}$$

Then according to the model the two dissipative scales are different. The definition given above is not

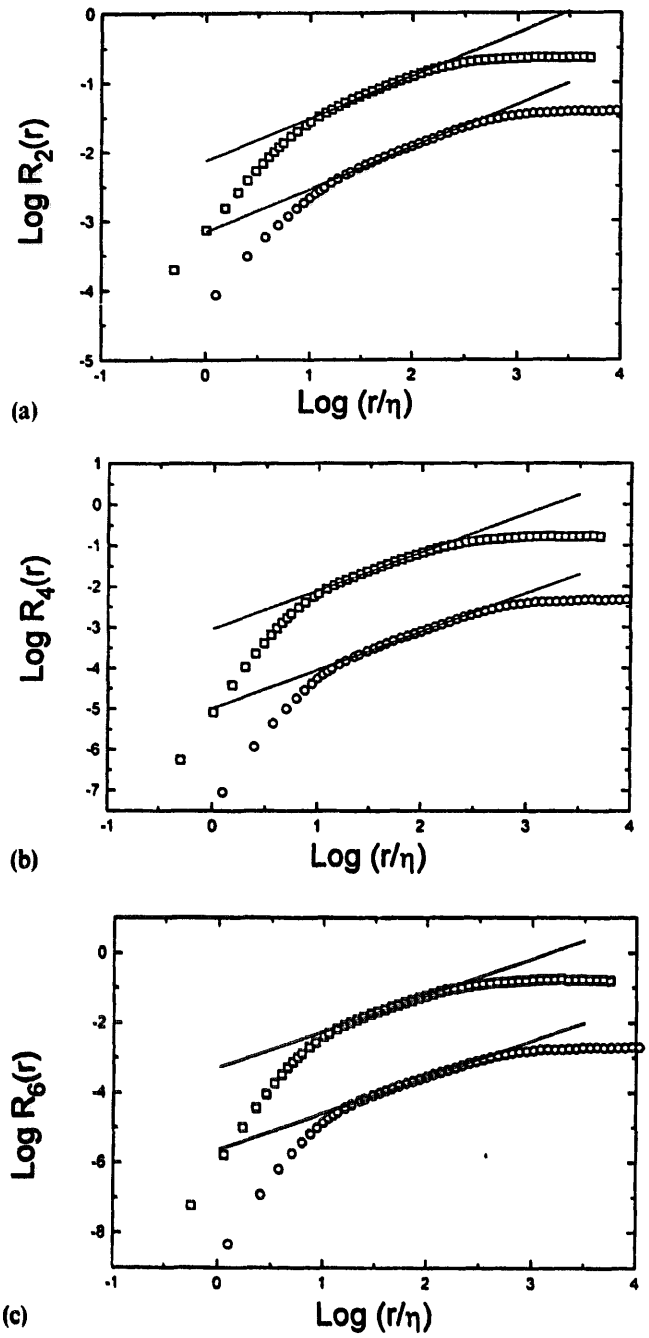

Fig. 1. Temperature structure functions at $Re = 9000$ (□), 35 000 (○): (a) R_2 vs. r/η, (b) R_4 vs. r/η and (c) R_6 vs. r/η. The straight lines have slopes equal to 0.62, 0.94 and 1.12, respectively.

the only possibility. In fact, there are other combinations of $\bar{\epsilon}$, χ and ν which have units of length and can be justified by simple physical arguments. Batchelor in a seminal work of 1958 [18] gives another estimate

$$\eta_\theta = \eta\, Pr^{-1}. \tag{9}$$

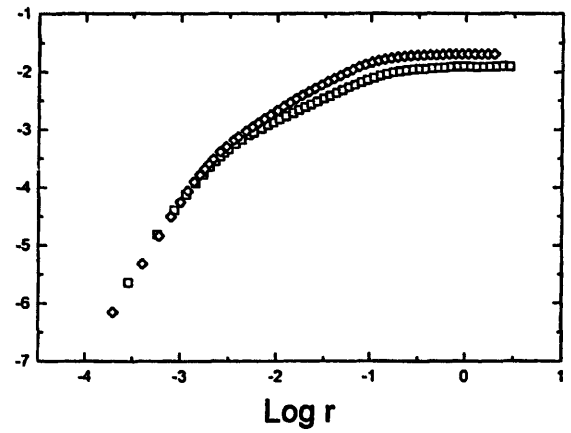

Fig. 2. Collapse of structure functions $R_3(r)$ (□) and $S_3(r)$ (◇) in the dissipative range. $Re = 35\,000$. The length scale for velocities was multiplied by 0.705. The behavior of the two functions in the dissipative range is essentially identical.

Recently Pumir [5] made a numerical study of the small scale structures in a passive scalar, finding that the dissipative scale for temperature is

$$\eta_\theta = 0.59\eta\, Pr^{-1/2}. \tag{10}$$

This equation has been checked numerically for $\frac{1}{8} < Pr < 1$ and $R_\lambda < 70$. In our experiment, using only one value of Pr, we cannot distinguish between Eqs. (8)–(10), but can check the numerical result by Pumir at higher R_λ. In order to do that we used the following procedure. The dissipative range is the interval where the temperature or velocity are smoothed by thermal diffussivity and viscosity, respectively, so the structure functions have a regular behavior, that is, $R_n(r) \propto r^n$ and $S_n(r) \propto r^n$. The key idea to experimentally evaluate the quotient η_θ/η is that in the vicinity of their corresponding dissipative scale the behavior of either temperature or velocity structure functions is essentially identical. Then, if the length scale for velocity is multiplied by a suitable factor both $R_n(r)$ and $S_n(r)$ must collapse in a single curve. The factor is precisely η_θ/η.

As an example we show in Fig. 2 the superposition of $R_3(r)$ with $S_3(r)$ in the dissipation range, obtained by multiplying the length scale for temperature by 0.71 for $Re = 35\,000$. In Table 1 the results obtained for two measurements are shown and compared with the described above models. As we can see, in our experiment it is found that $\eta_\theta \simeq 0.7\eta$ in agreement with

Table 1
Ratio η_θ/η of temperature to velocity dissipative scales

Model	η_θ/η
Monin–Yaglom	1.310
Batchelor	1.430
Pumir	0.705
Experiment ($Re = 9000$)	0.770
Experiment ($Re = 35\,000$)	0.710

Table 2
Exponents of the temperature and velocity structure functions

Order	$\xi(n)$	$\zeta(n)$
1	0.37 ± 0.003	0.37 ± 0.003
2	0.62 ± 0.005	0.70 ± 0.005
3	0.80 ± 0.008	1.00 ± 0.010
4	0.94 ± 0.010	1.28 ± 0.020
5	1.04 ± 0.010	1.54 ± 0.030
6	1.12 ± 0.020	1.78 ± 0.050
7	1.20 ± 0.020	2.00 ± 0.070
8	1.29 ± 0.020	2.23 ± 0.080

the numerical data by Pumir [5]. Of course this result is just an experimental check of the numerical data and it does not exclude the possibility of a different Prandtl dependence with another numerical prefactor. Other experiments with various Pr will be necessary in order to clearly check Eq. (10) at high Re.

4. Scaling exponents in the inertial range

The exponents of the temperature structure functions in the inertial range can be calculated with some accuracy from the data corresponding to the highest Reynolds number attained in our experiments. The structure functions $R_n(r)$ corresponding to $n = 2$, 4 and 6 are plotted vs. r/η in Fig. 1 in log–log scale. It is seen that the mean temperature differences decrease when Re increases, a phenomenon due to the fact that the amount of heat injected to the system remains the same while the volumetric flow increases when Re increases. In Table 2 the exponents of the temperature structure function are shown and compared with those of velocity. They are in agreement with previous measurements [19,20].

In the inertial range $L \gg r \gg \eta_\theta$ the Obukhov–Corrsin theory [7] predicts that $\xi(n) = \frac{1}{3}n$. However the passive scalar behavior show important deviations with respect to this law already for lower-order moments. This phenomenon is believed to be produced by a double intermittency correction, one related to the energy dissipation ϵ and the other to N. To take into account these effects the following scaling is proposed [20]:

$$R_n(r) \propto \langle \epsilon_r^{-n/6} N_r^{n/2} \rangle r^{n/3}, \tag{11}$$

where ϵ_r and N_r are the mean value on a volume of size r of the energy and temperature dissipation rate, respectively.

Another possibility is considered here, namely

$$R_n(r) \propto \langle \epsilon_r^{-n/6} \rangle \langle N_r^{n/2} \rangle r^{n/3}. \tag{12}$$

Both are in agreement with a dimensional analysis. In particular, Eq. (12) predicts that the second-order structure function is only affected by the intermittency in energy dissipation. This is the unique case where the intermittency does not contribute to the anomalous scaling. In order to compute ϵ_r and N_r we have used the one-dimensional surrogate, that is

$$\epsilon_r = \frac{\nu}{r} \int_x^{x+r} \left(\frac{\partial V(y)}{\partial y} \right)^2 \mathrm{d}y, \tag{13}$$

$$N_r = \frac{\chi}{r} \int_x^{x+r} \left(\frac{\partial \theta(y)}{\partial y} \right)^2 \mathrm{d}y. \tag{14}$$

In Fig. 3 the quotient $R_n(r)/\langle \epsilon_r^{-n/6} \rangle r^{n/3}$ is plotted for $n = 2$, 4 and 6. A plateau is recovered only for $n = 2$ showing that this is the unique value of n where the intermittency of N does not contribute to the anomalous scaling.

A test of Eqs. (11) and (12), described above, is given in Fig. 4, where $R_n(r)/\langle \epsilon_r^{-n/6} N_r^{n/2} \rangle r^{n/3}$ and $R_n(r)/\langle \epsilon_r^{-n/6} \rangle \langle N_r^{n/2} \rangle r^{n/3}$ are plotted as function of r for $Re = 35\,000$ and $n = 2$, 4 and 6. In both cases a plateau is recovered, but the ranges are slightly different. For $n = 2$ the correction introduced by the two models lead to exponents nearly identical, so at this level the experimental data are inconclusive. For the remaining moments the measurement gives also results not clearly different. This feature may be due to the use of relatively low-order structure functions or

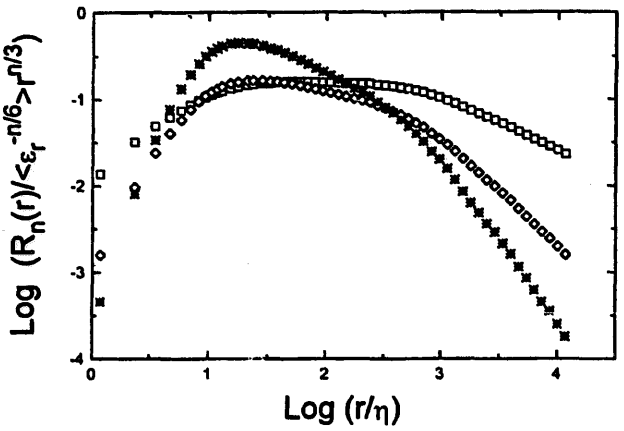

Fig. 3. Graph of $R_n(r)/\langle\epsilon_r^{n/6}\rangle r^{n/3}$ vs. r/η for $n = 2$ (□), 4 (◇) and 6 (∗). A plateau is recovered only for $n = 2$. The intermittency correction introduced by the energy dissipation does not suffice to explain the behavior of the temperature structure functions.

to a direct proportionality between both intermittency corrections.

Eq. (12) could be equivalent to the previous one only if the energy dissipation field and the temperature one are statistically independent. The question of the correlation between ϵ_r and N_r is treated in Fig. 5, where $\langle\epsilon_r^{-n/6}N_r^{n/2}\rangle$ is plotted vs. $\langle\epsilon_r^{-n/6}\rangle\langle N_r^{n/2}\rangle$ for three different values of n. In nearly all cases a straight line is attained, the slope being approximately 0.9. Only for $n = 2$ a slope equal to 0.8 is obtained. These values (near to 1) indicate a weak correlation between $N_r^{n/2}$ and $\epsilon_r^{-n/6}$.

The experimental finding that the second-order structure function is not affected by the intermittency in N may be put into the frame of a recent model developed by Benzi et al. [14]. After applying the random β model to the cascading of a passive scalar, they found that

$$R_2(r) \propto \overline{N} \cdot r \cdot \langle \delta V(r)^{-1} \rangle, \tag{15}$$

where $\delta V(r) = V(x+r) - V(x)$. A similar conclusion has been reached by Meneveau et al. [11]. Eq. (15) is in agreement with Eq. (12) after using the Kolmogorov refined similarity hypothesis. In order to test this model a negative structure function must be calculated which may pose some problems when dealing with experimental signals. Indeed, when digitized, two close velocity values can be stored as having the same

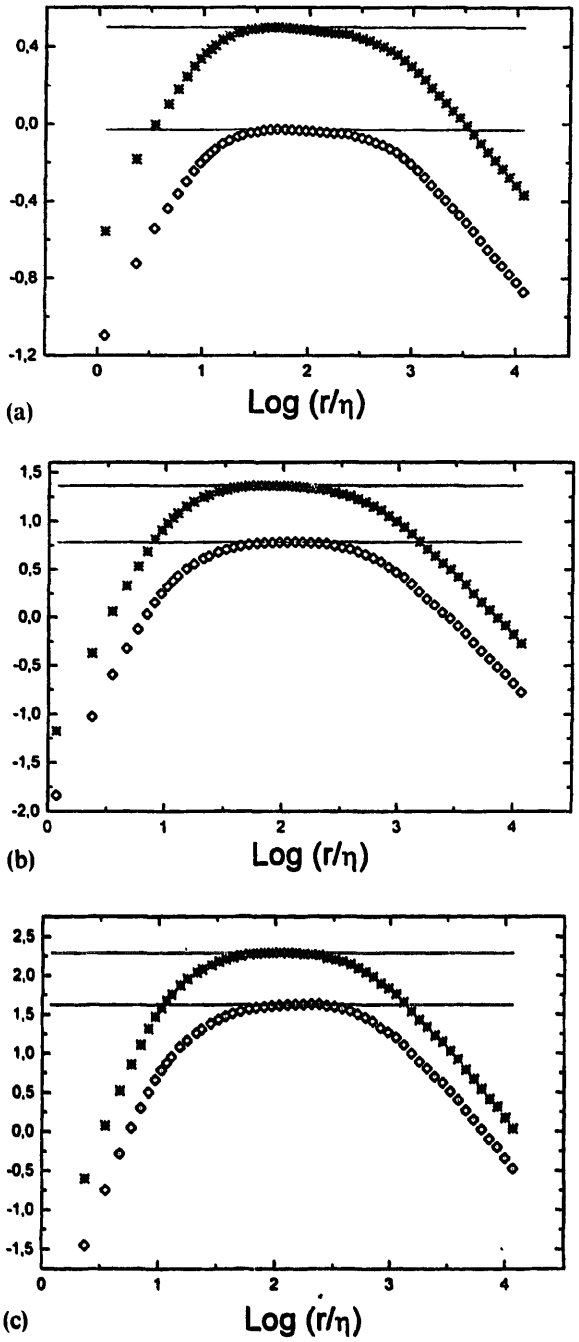

Fig. 4. Graph of $R_n(r)/\langle\epsilon_r^{-n/6}N_r^{n/2}\rangle r^{n/3}$ (∗) and $R_n(r)/\langle\epsilon_r^{n/6}\rangle\langle N_r^{n/2}\rangle r^{n/3}$ (◇) vs. r/η for $Re = 35\,000$: (a) $n = 2$, (b) $n = 4$ and (c) $n = 6$. A plateau is obtained with both intermittency corrections, but the ranges are slightly different.

magnitude, producing in this way a spurious $\delta V(r) = 0$ and a singular point for $\delta V(r)^{-1}$. The question is how to skip these singular points when the negative moment is numerically computed.

A way to avoid this problem is to use the generalization of the refined Kolmogorov similarity hypothesis

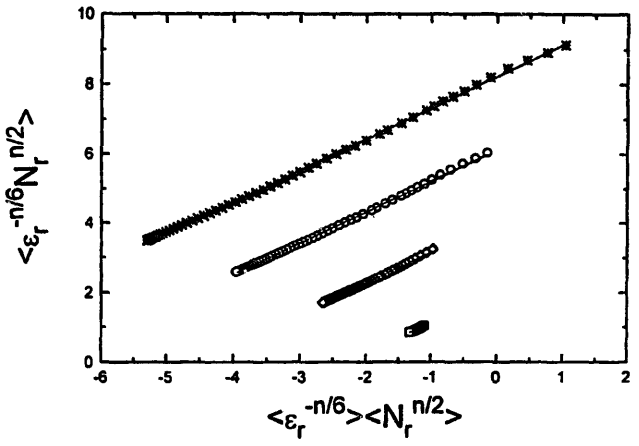

Fig. 5. Graph of $\langle \epsilon_r^{-n/6} N_r^{n/2} \rangle$ vs. $\langle \epsilon_r^{-n/6} \rangle \langle N_r^{n/2} \rangle$ for $n = 2$ (□), 4 (◇), 6 (○) and 8 (∗) at $Re = 35\,000$. The straight lines correspond to the best fit. The slopes are close to 0.9, except for $n = 2$, where the slope is 0.8. This implies that the correction introduced by $\langle \epsilon_r^{-n/6} N_r^{n/2} \rangle$ is smaller if compared to those of $\langle \epsilon_r^{-n/6} \rangle \langle N_r^{n/2} \rangle$. On the other hand, the values of the slopes (near to the unity) imply that ϵ_r and N_r have a weak correlation.

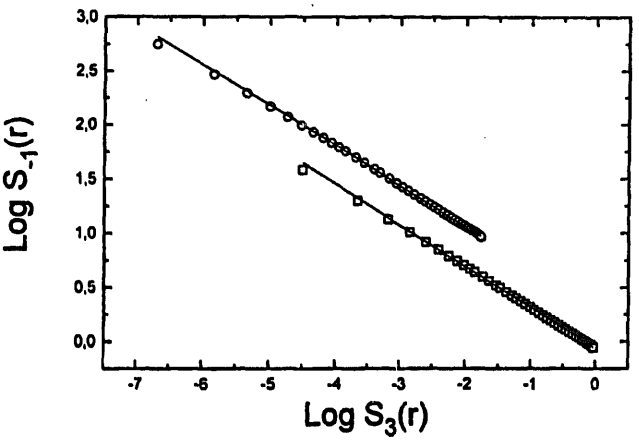

Fig. 6. Structure function $S_{-1}(r)$ vs. $S_3(r)$. The straight lines are the best fit at $S_3(r)^{-0.38}$, for $r > 5\eta$.

stated in a previous paper [21]. The -1 order structure function can be expressed as

$$|\langle \delta V(r)^{-1} \rangle| \propto \langle \epsilon_r^{-1/3} \rangle S_3(r)^{-1/3}. \tag{16}$$

The right-hand side includes the average of a quantity to a negative power, but this is not a disadvantage because ϵ_r is the integral of ϵ, a non-negative quantity. ϵ may be zero at some point, but its integral over a finite interval is always positive.

The calculation of exponent $\zeta(-1)$ is performed by using the idea of ESS. In Fig. 6 $|\langle \delta V(r)^{-1} \rangle|$ is plotted vs. $\langle |\delta V(r)|^3 \rangle$. In a broad range the data satisfy a power law behavior with an exponent $\zeta(-1) = -0.38 \pm 0.01$. Then it may be stated that $\xi(2) = 0.62 \pm 0.01$ which is in agreement with the value given in Table 2. Notice that the intermittency correction given in Eq. (14) has the opposite sign with respect to those of the velocity because $\zeta(-1) < -\frac{1}{3}$.

5. Extended self-similarity

It is usually very difficult to get an accurate statistical estimate of $\zeta(n)$ and $\xi(n)$ because clear scaling laws are observed in structure functions only at large Re. It has been recently shown that the scaling properties of velocity structure functions can be extended almost to dissipative scaling [15] in the following way:

$$S_n(r) = A_n S_3(r)^{\zeta(n)}. \tag{17}$$

This property which holds for $r > 5\eta$ has been named ESS and it allows to have a much better estimate of $\zeta(n)$ even at small Re.

One of the purpose of this paper is to experimentally show that ESS holds also for R_n, that is

$$R_n(r) = A_{n,m} [R_m(r)]^{\beta(n,m)}, \tag{18}$$

where $\beta(n, m) = \xi(n)/\xi(m)$.

In Fig. 7 the R_n for $n = 4$ and 6 are shown as function of R_2 whose exponent is $\xi(2) = 0.62$. In looking at Fig. 7 we observe that the scaling region is wider than that of Fig. 2, even at small Re. Within experimental errors we find that $\beta(n, 2)$ does not depend on Re. The vlaues of the exponents are

$$\xi(n) = \beta(n, 2) \cdot 0.62. \tag{19}$$

There are several important differences between Eqs. (17) and (18). In Eq. (17) the natural reference function is S_3 because the Kolmogorov equation imposes $|\langle \delta V(r)^3 \rangle| \propto\in r$ for r in the inertial range. In contrast in Eq. (18) the natural reference function would be $D_{VTT} = \langle \delta V(r) \delta\theta(r)^2 \rangle$, which scales as r in the inertial range [6]. However, as we have seen, the scalar and velocity have in general different dissipation scales and thus the scaling range of the $R_n(r)$ is not extended if they are drawn as a function of D_{VTT} because this one is a mixed moment.

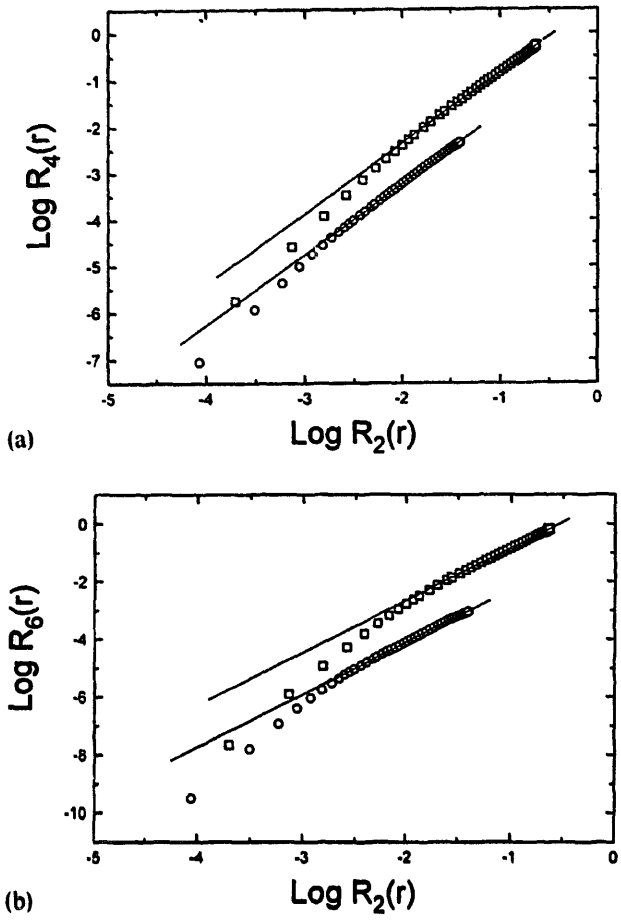

Fig. 7. Temperature structure functions (a) R_4 and (b) R_6, drawn as a function of R_2. The same symbols as in Fig. 2 have been used for the different Re. The slopes of the solid lines are 1.52 for R_4 and 1.79 for R_6. Then the values of the exponents $\xi(n)$ are, respectively, 0.94 and 1.11.

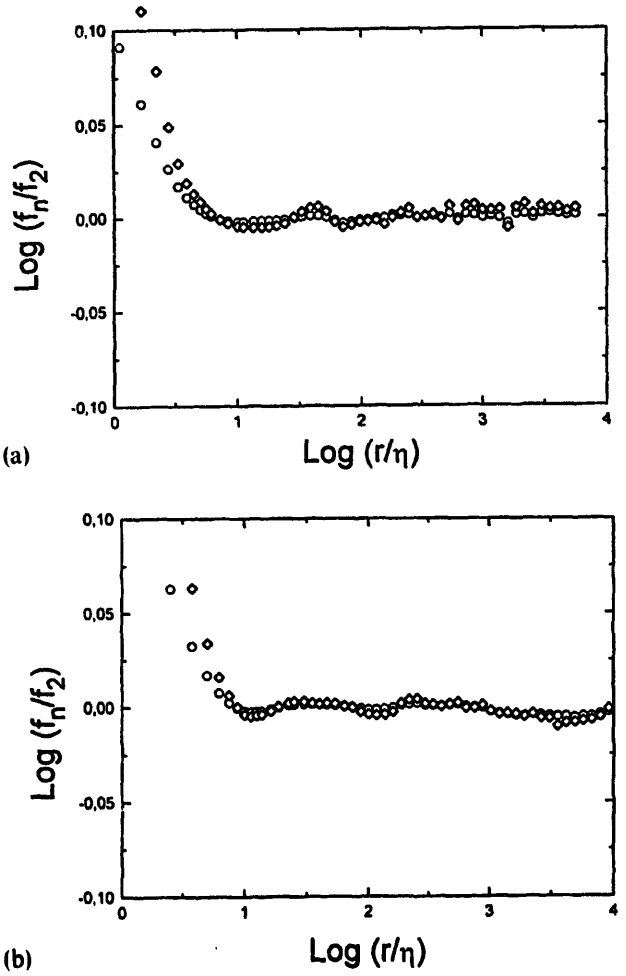

Fig. 8. The ratios of the universal functions f_4/f_2(○) and f_6/f_2(◇): (a) $Re = 9000$ and (b) $Re = 35000$. ESS holds for $r > 5\eta$.

Here we want to focus only on the fact that R_2 can be used as a reference structure function because we experimentally show that its scaling is not affected by the intermittency of N and also because the exponent $\xi(2)$ have the same value if calculated following different ways. The values computed using Eq. (19) are compared with the values computed directly from the scaling of R_n vs. r at the highest Re number. We see that the values computed with the two methods coincide within error bars. This shows that ESS holds also for the structure functions of temperature as for those of velocity.

Finally let us discuss the range of r where the concept of ESS can be applied to R_n. In the case of the S_n we know that this range extends till $r \simeq 5\eta$ [15]. The best way of doing this is to use a consequence of ESS. Indeed Eq. (17) implies the existence of a universal function such that all the $S_n(r)$ can be expressed in the following way:

$$S_n(r) = A_n \left[\frac{r}{L} f\left(\frac{r}{\eta}\right)\right]^{\zeta(n)}, \tag{20}$$

where A_n is a normalization constant and $f(r/\eta) = 1$ for r in the inertial range. The existence of this universal function can be checked by computing

$$f_n(r) = \frac{L \cdot S_n^{1/\zeta(n)}}{r} A_n^{-1/\zeta(n)}.$$

In Fig. 8 we report the ratios f_6/f_2 and f_4/f_2 as a function of r/η. We notice that the ratios remain constant within 2% for $r \geq 5\eta$ meaning that the $f_n \sim f$

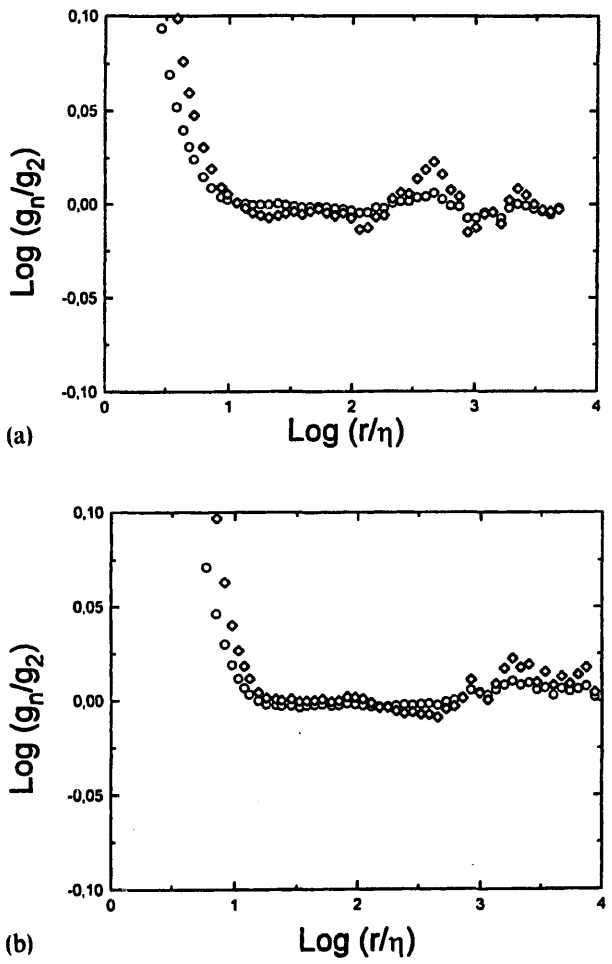

Fig. 9. The ratios of the universal functions g_4/g_2 (○) and g_6/g_2 (◇): (a) $Re = 9000$ and (b) $Re = 35000$. ESS holds on a narrower range (approximately for $r > 7\eta$).

for all n with a 2% accuracy. We have applied the same check to the R_n. Specifically we have computed

$$g_n(r) = \frac{L \cdot R_n^{1/\xi(n)}}{r} B_n^{-1/\xi(n)}. \tag{21}$$

In Fig. 9 we report the ratios g_6/g_2 and g_4/g_2. We also see that in this case the ratios remain constant on a wide range which however is more limited than for the f_n. The reason for this difference is not clear. In Section 3 we have seen that $\eta_\theta < \eta$ (see Table 1). Thus the different cutoff between velocity and temperature cannot be at the origin of the different behavior of $g(r)$ and $f(r)$ observed in Figs. 8 and 9.

6. Hierarchy of the temperature structure function

Recently She and Lêveque [16] developed a model according to which the turbulence consists of a set of structures with many degrees of coherence, going from random to filamentary vortex. The authors suggest the existence of a relation among different moments of ϵ_r, that is

$$\frac{\langle \epsilon_r^{p+1} \rangle}{\langle \epsilon_r^p \rangle} = C_p \left(\frac{\langle \epsilon_r^p \rangle}{\langle \epsilon_r^{p-1} \rangle} \right)^\beta \epsilon_r^{(\infty)(1-\beta)}, \tag{22}$$

where C_p are geometrical constants and $\epsilon_r^{(\infty)} = \lim_{p\to\infty} \langle \epsilon_r^{p+1} \rangle / \langle \epsilon_r^p \rangle$ is associated in [16] to the filamentary structures of the flow. On the basis of simple arguments it is assumed that $\epsilon_r^{(\infty)} \propto r^{-2/3}$ and $\beta = \frac{2}{3}$. This relation has been experimentally verified. The last equation can be transformed in a relation among structure functions by using the Kolmogorov refined similarity hypothesis [21]. The result is [22]:

$$\frac{S_{n+1}(r)}{S_n(r)} = D_n \left(\frac{S_n(r)}{S_{n-1}(r)} \right)^{\beta'} F(r)^{(1-\beta')}, \tag{23}$$

where $\beta' = \beta^{1/3}$ and $F(r)$ is a function independent of n.

This section is intended to build a relation for temperature structure functions, based on the same idea of She and Lêveque. First we assume that the functions $R_n(r)$ satisfy the following equation:

$$\frac{R_{n+1}(r)}{R_n(r)} = E_n \left(\frac{R_n(r)}{R_{n-1}(r)} \right)^\alpha (G(r))^{(1-\alpha)}, \tag{24}$$

where $G(r) = \lim_{n\to\infty} R_{n+1}(r)/R_n(r)$ is independent of n and it is determined, as in the original She and Lêveque model, by the most intermittent structures. Let us assume that $G(r) \propto r^{\Delta_\infty}$. If Eq. (24) is recursively applied, we obtain that the exponent of the n-order structure function is expressed in terms of $\xi(1)$, $\xi(2)$ and α:

$$\xi(n) = \Delta_\infty n + C(1 - \alpha^n), \tag{25}$$

where

$$C = \frac{\xi(1)}{1-\alpha} - \frac{\xi(2) - (1+\alpha)\xi(1)}{(1-\alpha)^2}$$

and

$$\Delta_\infty = \frac{\xi(2) - (1+\alpha)\xi(1)}{(1-\alpha)}.$$

In the original model [16] C is the codimension of the most intermittent structures (see also [23,24]). In order to evaluate the exponents of the structure functions with the latter equation we need to know three quantities. If we take $\xi(1) = 0.37$ and $\xi(2) = 0.62$, the parameter α can be adjusted to obtain a fit with the remaining exponents. The value obtained with this procedure is $\alpha = 0.62$. However, the parameter α can be evaluated directly from Eq. (24). To do so, we follow the same procedure we have used in order to test Eq. (22) [25]. We make the quotient of Eq. (24) evaluated at r and the same equation evaluated at r'. The reason for doing this quotient is to obtain a relation where the E_n does not appear. We obtain

$$Y_{n+1}(r,r') = \alpha[Y_n(r,r')] + (1-\alpha)\log\left[\frac{G(r)}{G(r')}\right], \tag{26}$$

where

$$Y_{n+1}(r,r') = \log\left[\frac{R_{n+1}(r)R_n(r')}{R_n(r)R_{n+1}(r')}\right].$$

By studying the dependence of Y_{n+1} as a function of Y_n at various n and fixed r, r' one can easily determine the value of α, because the ratio $G(r)/G(r')$ does not depend on n. In Fig. 10 Y_{n+1} is plotted as a function of Y_n for $1 < n < 6$, at fixed r, r' whose values are quoted in the caption. We clearly see that the data are on straight lines of slope α, which has a mean value of 0.63. This value is close to that found from the fit made using $\xi(n)$ and Eq. (25). Both results are close to $\frac{2}{3}$ which could be the correct one. A conclusive reply could be done with further experiments and the construction of a new model based on the existence of structures with many degrees of coherence. Once α is known from Eq. (24) with $n = 1$ one can first compute

$$G(r) = \left[\frac{R_2(r)}{R_1(r)^{1+\alpha}}\right]^{1/(1-\alpha)}.$$

Finally Eq. (24) can now be directly checked by plotting for a fixed value of n the first terms as a function

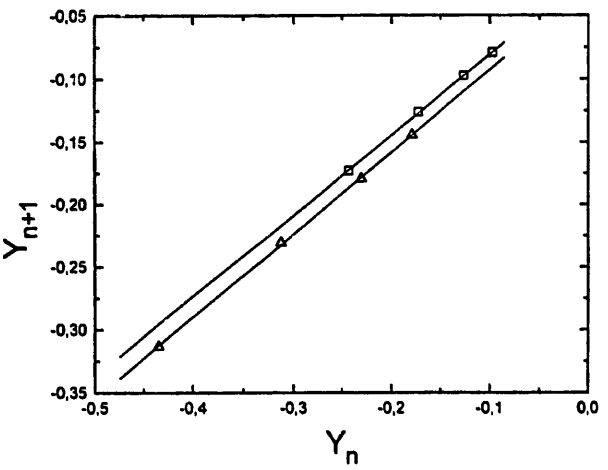

Fig. 10. Graph of Y_{n+1} vs. Y_n for $1 < n < 6$ at fixed r and r'. In the figure two different pairs of r and r' are used: (△) $\log r = -2.54$, $\log r' = -1.1$, (□) $\log r = -1.97$, $\log r' = -1.1$. $Re = 35\,000$. The slopes are 0.63 ± 0.01.

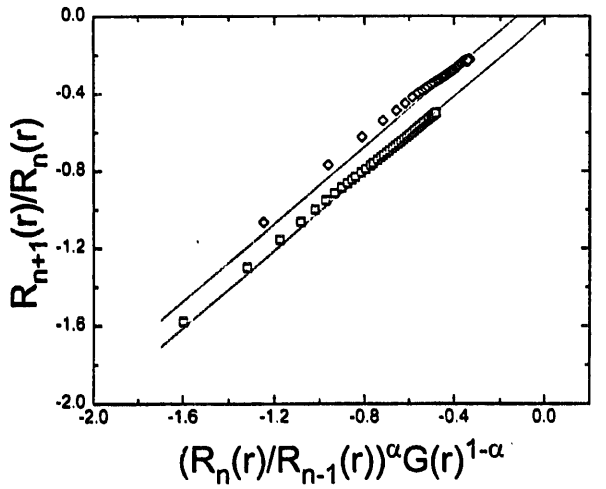

Fig. 11. Graph of $R_{n+1}(r)/R_n(r)$ vs. $(R_n(r)/R_{n-1}(r))^\alpha (G(r))^{(1-\alpha)}$ for $n = 2$ (□) and $n = 5$ (◇) $Re = 35\,000$. The data are aligned on straight lines with slope near to 1. A jump is observed near the dissipative scale.

of the second. This is done in Fig. 11. We clearly see that the data are aligned on straight lines with slope close to 1. However the scaling does not extend continuously from large to small scales as it happens for Eq. (23) for the velocity field. A jump is observed. This is another important difference between the scalar and the velocity fields.

These checks confirm that the hierarchy of Eq. (24) is compatible with experimental data. However, we need to relate the value of α to some physical quan-

tity. With $\alpha = 0.63$, $\xi(1) = 0.37$ and $\xi(2) = 0.62$ we find $C = 0.8 \pm 0.1$ and $\Delta_\infty = 0.06 \pm 0.02$. As we said before, C is the codimension of the most intermittent structures of the flow. This means that the dimension of these objects is 2.2 ± 0.1. This value suggests that the most intermittent structures, related to $G(r)$, are not filaments as in the velocity field, but convoluted sheets. This result agrees with those of previous works on passive scalars. Indeed Pumir [5] has shown the existence of steep scalar fronts separating well mixed regions. Then the most intermittent structures are objects of dimension close to 2. On the other hand, Sreenivasan [26] shows that the interface of a scalar introduced in a flow has a dimension equal 2.36 which gives a codimension close to C. Thus our value of α correctly estimates the codimension of the most intermittent structures of the flow.

In contrast we were unable to find any reasonable physical arguments able to predict the value of Δ_∞ as it has been done in the original She and Lêveque model. Things are indeed much more complex because two dissipation fields have to be considered. This will be the object of further investigation.

7. Conclusions

In this paper some characteristics of a passive scalar were experimentally studied. First, it was found that dissipative scale for temperature is smaller than the corresponding quantity for velocity. Moreover, an agreement with numerical simulations by Pumir was found. On the other hand, the scaling exponents in the inertial range were calculated and a detailed revision of the intermittency corrections was made. Two corrections of the temperature structure functions were taken into account, both including intermittencies of ϵ and N. At this level the experimental data are inconclusive because both corrections are not very different. We have also verified that the conjecture of [8] about the exponent of the second-order temperature is compatible with experimental data.

Another point was treated in this paper, that is, the applicability of ESS to a passive scalar. A broader power law behavior is detected when $R_n(r)$ is plotted vs. $R_2(r)$. However, the extended inertial range begin not at $r = 5\eta$ as in the velocity statistics, but at $r = 7\eta$.

Finally, a hierarchy for the temperature structure functions was built. Following the ideas of She and Lêveque, a relation among structure functions was proposed. The intermittency correction based on these ideas agrees within error bars with the experimental measurements and correctly predicts the codimension of the most intermittent structures of a passive scalar.

Acknowledgements

We acknowledge useful discussion with R. Benzi and A. Pumir. This work has been partially supported by EEC contract No. ERBCHRXCT940546 and DRET contract No. 942555.

References

[1] Villermeaux and Y. Gagne, Phys. Rev. Lett. 73 (1994) 252.
[2] S. Vaienti, M. Ould-Rouis, F. Anselmet and P. Le Gal, Physica D 73 (1994) 99.
[3] M. Old-Rouis, F. Anselmet, P. Le Gal and S. Vaienti, Physica D 85 (1995) 405.
[4] B. Castaing, Physica D 73 (1994) 31.
[5] A. Pumir, Phys. Fluids 6 (1994) 3974.
[6] A.S. Monin and A.M. Yaglom, Statistical Fluid Mechanics (MIT Press, Cambridge, MA, 1975).
[7] A.M. Obukhov, Izv. Akad. Nauk SSSR Ser. Geogr. Geofiz. 13 (1949) 58; S. Corrsin, J. Appl. Phys. 22 (1951) 469.
[8] Jayesh and Z. Warhaft, Phys. Rev. Lett. 67 (1991) 3503.
[9] R.R. Prasad, C. Meneveu and K.R. Sreenivasan, Phys. Rev. Lett. 61 (1988) 74.
[10] F. Anselmet, Y. Gagne, E.J. Hopfinger and R.A. Antonia, J. Fluid Mech. 140 (1984) 63.
[11] C. Meneveu, K.R. Sreenivasan, P. Kailasnath and S. Fan, Phys. Rev. A 41 (1990) 894.
[12] S. Vainshtein, K.R. Sreenivasan, R.T. Pierrehumbert, V. Kashiap and A. Juneja, Phys. Rev. E 50 (1994) 1823.
[13] A.N. Kolmogorov, Dokl. Akad. Nauk SSSR 30 (1941) 301.
[14] R. Benzi, L. Biferale and G. Parisi, Europhys. Lett. 18 (1992) 213.
[15] R. Benzi, S. Ciliberto, C. Baudet and G. Ruiz Chavarria, Physica D 80 (1995) 385.
[16] S.-Z. She and E. Lêveque, Phys. Rev. Lett. 72 (1994) 336.
[17] Z. Warhaft and J.L. Lumley, J. Fluid Mech. 88 (1978) 659.
[18] G.K. Batchelor, J. Fluid Mech. 5 (1959) 113.

[19] R. Antonia, E. Hopfinger, Y. Gagne and F. Anselmet, Phys. Rev. A 30 (1984) 2704.
[20] R.A. Antonia and C.W. Van Atta, J. Fluid. Mech. 84 (1984) 561.
[21] G. Ruiz Chavarria, J. Phys. II (France) 4 (1994) 1083.
[22] G. Ruiz Chavarria, C. Baudet, R. Benzi and S. Ciliberto, J. Phys. II (France) 5 (1995) 485.
[23] B. Dubrulle, Phys. Rev. Lett. 73 (1994) 959.
[24] B. Dubrulle, Europhys. Lett. submitted.
[25] G. Ruiz Chavarria, C. Baudet and S. Ciliberto, Phys. Rev. Lett. 74 (1995) 1986.
[26] K.R. Sreenivasan, Ann. Rev. Fluid Mech. 23 (1991) 539.